Pressure-Dependent Decomposition Kinetics of the Energetic Material HMX up to 3.6 GPa

Elizabeth A. Glascoe,* Joseph M. Zaug, and Alan K. Burnham

Lawrence Livermore National Laboratory, 7000 East Avenue, Livermore, California 94551

Received: June 4, 2009; Revised Manuscript Received: September 10, 2009

The effect of pressure on the global thermal decomposition rate of the energetic material HMX was studied. HMX was precompressed in a diamond anvil cell (DAC) and heated at various rates. The parent species population was monitored as a function of time and temperature using Fourier transform infrared (FTIR) spectroscopy. Global decomposition rates were determined by fitting the fraction reacted to the extended-Prout−Tompkins nucleation−growth model and the Friedman isoconversional method. The results of these experiments and analysis indicate that pressure accelerates the decomposition at low-to-moderate pressures (i.e., between ambient pressure and 0.1 GPa) and decelerates the decomposition at higher pressures. The decomposition acceleration is attributed to pressure-enhanced autocatalysis, whereas the deceleration at high pressures is attributed to pressure-inhibiting bond homolysis step(s), which would result in an increase in volume. These results indicate that both the β- and δ-polymorphs of HMX are sensitive to pressure in the thermally induced decomposition kinetics.

Introduction

The role of pressure in the thermal decomposition mechanisms and kinetics of solid-state energetic materials is an interesting and important topic. Pressure can accelerate heterogeneous and gas-phase reactions and can inhibit reactions that involve an increase in volume. Such competing effects make it difficult to predict the role of pressure without a detailed knowledge of the decomposition mechanism of a material. The pressure-dependent kinetics of thermal decomposition are of great importance to the assessment and prediction of thermal safety of energetic materials because pressure is a dynamic variable in any sealed container that is heated. This work describes pressure-dependent kinetics of the thermal decomposition of the energetic material, HMX (octahydro-1,3,5,7-tetranitro-1,3,5,7-tetrazocine), between ambient pressure and 3.6 GPa.

HMX has been studied and used in a wide range of explosives and propellants for at least 60 years; therefore, there is a solid foundation of literature describing its thermal decomposition mechanisms. Most studies indicate that the decomposition begins with either N-NO_2 bond homolysis or HONO formation, although other initiation mechanisms have been observed.[1−4] The initial products of HMX molecular decomposition attack the unreacted HMX molecules and intermediates, producing a variety of autocatalytic reactions.[3,4] The mechanisms and kinetics of HMX decomposition are described, in detail, in the literature.[1−11]

Although many aspects of the HMX decomposition mechanism are established, the effect of pressure is poorly understood. There exist only a few kinetic studies of solid-state HMX decomposition at elevated pressures, and a comparison of the results raises many questions. Burnham et al. monitored the decomposition of HMX using differential scanning calorimetry (DSC) between ambient pressure and 1000 psi (7×10^{-3} GPa) and found that HMX decomposition accelerates as a function of pressure.[8] However, Piermarini et al. found exactly the opposite trend when HMX was decomposed at higher pressures (ca. 3−6 GPa) in a diamond anvil cell (DAC).[9] There are two major differences between these two studies, which might explain the contradicting trends: the polymorph of HMX as it undergoes molecular decomposition and the method of monitoring the decomposition. In Burnham's DSC results, HMX decomposed from the δ-polymorph and is monitored via the heat flow produced from the chemical reactions. In Piermarini's DAC experiments, HMX decomposed from the β-polymorph, and the population of HMX is monitored directly using FTIR spectroscopy. On the basis of these two studies, it is unclear what role pressure plays in the decomposition of HMX and whether the polymorph of HMX affects the decomposition rate.

Previous studies have provided limited insight into the role of the polymorph in the decomposition or deflagration of HMX, largely because many of the studies are not probing simple chemical systems. Rather, they are investigating inhomogeneous materials (e.g., plastic bonded explosives) that may have undergone various material transformations. For example, pressure-dependent deflagration studies up to several hundred megapascals report that plastic-bonded explosives burn much faster after undergoing a $\beta \rightarrow \delta$ transition.[12] However, the acceleration is probably not due to an intrinsic molecular decomposition rate in different polymorphs. Instead, a more likely reason for this acceleration in deflagration is improved penetration of the decomposition flame into cracks caused by the volume expansion during the $\beta \rightarrow \delta$ transition.[12] Slow cook-off thermal explosion experiments provide no consistent trend from one material to the next concerning the violence of the β- versus the δ-polymorph of the explosives.[13] However, these cook-off experiments have multiple variables associated with the confinement of a large plastic-bonded explosive under thermal stress (e.g., temperature, confinement pressure, thermal transport mechanisms, material deconsolidation, porosity, binder mechanical properties, etc.) that can influence the violence of deflagration, making isolation of an intrinsic chemical reactivity difference related to the polymorph difficult or impossible. Isothermal heating time-to-explosion studies indicate that raising the pressure from 1 to 5 GPa increases the explosion time by a factor of three.[11] This result is qualitatively consistent with

* To whom correspondence should be addressed. E-mail: glascoe2@llnl.gov.

10.1021/jp905276k CCC: $40.75
Published on Web 10/14/2009

Piermarini et al.'s findings[9] but quantitatively different, most likely because of the methods of detection and the more complex thermal transport mechanisms involved in a thermal explosion versus a thermal decomposition. A study that is focused on simply the reactions kinetics of the polymorph without the additional variables present in these multivariable cook-off and thermal explosions studies is needed and would assist in the interpretation of these previous studies.

In this work, the decomposition kinetics of either β- or δ-HMX are studied from ambient pressure up to 3.6 GPa through the combination of DAC techniques and Fourier transform infrared (FTIR) spectroscopy. In this study, we monitor the population of crystalline β- and δ-HMX molecules as a function of pressure and temperature and determine the kinetics of their disappearance. Our kinetics serve as an indicator of the global decomposition kinetics of HMX; no other transient species, polymorphs, or phases (e.g., liquid or gas) of HMX could be observed via our 1 min time resolution and instrument sensitivity. By studying the kinetics at pressures identical to those of both Burnham et al.[8] and Piermarini et al.[9] as well as pressures that span between the two regimes, the opposing trend of the DSC and DAC results is resolved. The role of the HMX polymorph is explored, and the pressure-dependent kinetics of HMX decomposition are reported.

Experimental Section

Sample. HMX powder, manufactured by Holston Army Ammunition Plant (Hol 6HBFC21-25. LLNL no. B-881), was reduced to a grain size of ca. 3 μm via fluid energy milling at Lawrence Livermore National Laboratory. In all experiments, HMX powder was sandwiched between cesium iodine (CsI) windows and packed into a DAC sample chamber. The CsI protected the diamonds from highly reactive decomposition products and transmitted applied pressure. Strontium tetraborate was used as a pressure manometer[14] and was placed between the CsI window and the diamond culets so as to avoid chemical reactions with the decomposing HMX. The DAC sample cavity consisted of two counter-opposed 400 μm diameter, type II diamond culets and a preindented 50−70 μm thick Inconel foil gasket. The chamber diameter is cut using a microelectric discharge machine (Hylozoic Products) and is nominally 100 μm. HMX sample mass used in these experiments is estimated to be on the order of micrograms or less and HMX sample thickness is <10 μm.

Instrument. The decomposition of HMX was monitored in situ via FTIR spectroscopy. The FTIR instrument was specially designed and built in-house to achieve the high spatial resolution that is necessary for monitoring small samples within the DAC; a detailed description of the instrument was previously described.[15] In brief, a mid-IR glowbar source is focused to a diameter of ca. 1 mm, transmitted through a sample, and focused into a cryogenically cooled single-element InSb−HgCdTe sandwich detector. Two irises are situated along the beam path before and after the sample to enable >30 μm spatially resolved IR absorption measurements; however, in these experiments, we typically filled the entire sample chamber to increase our signal-to-noise ratio. A Bruker Optics Vector 33 interferometer is used to collect 2 cm^{-1} resolution data between 400 and 5000 cm^{-1}. When averaging 15 interferograms (preselected to optimize signal-to-noise), the instrument response time is ~1 min, and spectra were collected every minute; consequently, only the kinetics of parent molecule depletion and final product formation were monitored. Background spectra of the diamond and CsI window material were collected prior to loading samples.

Decomposition Experiments. The sample was heated via a resistive heater ring (Watlow) attached to the outer circumference of the DAC. Thermal ramping was controlled using a high stability temperature and process control unit (Eurotherm 2400 series). The sample/cell temperature in all experiments was monitored with a K-type thermocouple mounted at the diamond table. For calibration purposes, a second thermocouple was mounted on the interior diamond facet, near the diamond culet (and therefore closer to the sample than the diamond table). Multiple controlled tests demonstrated that the temperature readings at these two locations varied linearly with the heater temperature and at the highest temperature studied (320 °C), they differed by 22 °C; therefore, we applied a linear adjustment to our table-mounted thermocouple. Presumably, the temperature near the HMX sample is higher because of the insulation properties of the CsI windows between the HMX and the diamond. We determined fine calibration of the temperature disparity between the sample and the diamond table thermocouple by comparing the HMX polymorph transformation (i.e., $\beta \rightarrow \delta$) temperature measured in the DAC and that measured using DSC at the same heating rate. The linear relationship was adjusted to account for the differences between the DSC and DAC temperatures for the $\beta-\delta$ transformation. This fine calibration resulted in an additional adjustment of 8 °C at the highest temperatures (ca. 350 °C), and no difference in temperature at the lowest temperatures (ca. 25 °C). All experiment temperatures were monitored via the thermocouple on the diamond table and adjusted according to the same linear function; therefore, the temperature calibration was the same for all experiments and is a systematic adjustment that will not change the results relative to each other.

In a typical experiment, HMX and CsI were loaded into the DAC and uniaxially compressed to a target pressure. The DAC was mounted into the heating ring and aligned to the FTIR microscope. In the isothermal experiments, the sample was rapidly heated to the desired temperature and held constant. In the thermal ramp experiments, the sample was rapidly heated to a moderate temperature (135−170 °C depending on the pressure), allowed time to equilibrate (ca. 10 min), and heated further at a rate of either 0.5 or 0.25 °C/min. During the temperature equilibration period and periodically during the ramped heating phase, the sample pressure was monitored and adjusted, in situ, as needed to maintain a constant pressure throughout each experiment.

Pressure was determined via the calibrated fluorescence wavelength shift of strontium tetraborate and maintained, in situ, with the use of a gas-actuated metal-membrane attached to the DAC. All experiments at $P \geq 1$ GPa were maintained at a constant pressure to within ca. 0.1 GPa prior to decomposition. During decomposition the pressure increased by ca. 0.40 GPa, presumably, because of the formation of product gases. In the ambient pressure experiments, a small void was left between the diamond and the CsI to allow for gas expansion without a pressure rise. No pressure measurements were made for the ambient pressure experiments; instead the temperature for the $\beta \rightarrow \delta$ transition was used to verify ambient pressure conditions. The reported pressures in the experiments between 0 and 1 GPa were estimated on the basis of limited pressure measurements and the $\beta \rightarrow \delta$ transition temperature.[16]

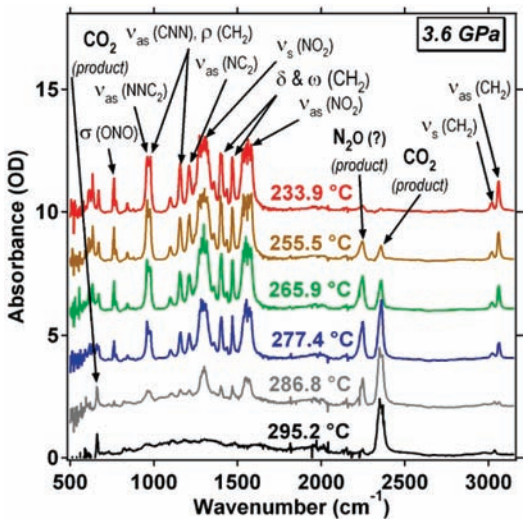

Figure 1. Infrared absorption spectra for β-HMX decomposition at 3.6 GPa during a ramped heating experiments (0.5 °C/min). Spectra baselines were vertically shifted for easy visualization.

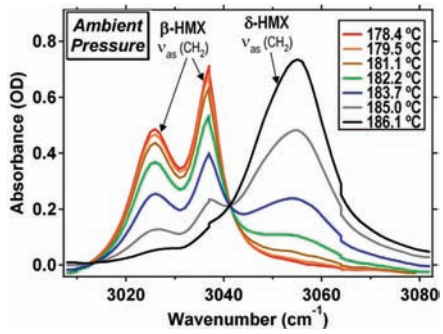

Figure 2. Infrared absorption spectra showing the conversion of β-HMX to the δ-polymorph under ambient pressure during a ramped heating experiments (0.5 °C/min).

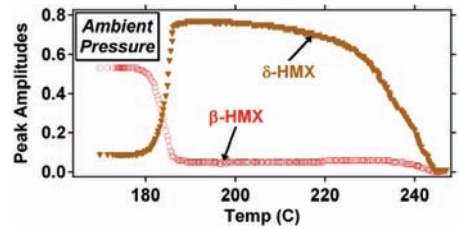

Figure 3. Infrared peak amplitude for the 3026 and 3055 cm^{-1} peaks (asymmetric CH_2 stretch of HMX in β- and δ-polymorph, respectively) under ambient pressure during a ramped heating experiments (0.5 °C/min).

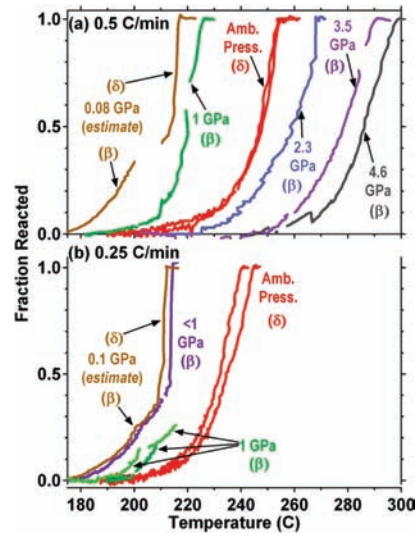

Figure 4. Fraction of HMX decomposed at various pressures at (a) 0.5 and (b) 0.25 °C/min heating rate. The polymorph of HMX (β or δ) is labeled for each curve. In the case of the 0.08 and 0.1 GPa decomposition, HMX began to decompose in β-form and then underwent $\beta-\delta$ polymorph transition and completed the decomposition in δ-form. Under all other pressures, the decomposition was exclusively in a single polymorph.

Results

Spectral Analysis. Figure 1 shows the infrared spectrum of HMX at 3.6 GPa between 233.9 and 295.2 °C during a 0.5 °C/min ramp. HMX peak assignments are provided in the literature.[17] At this pressure, the $\beta \rightarrow \delta$ transition is inhibited;[9] consequently, HMX is observed to decompose from the β-polymorph, and no δ-HMX is observed. All of the experiments at $P \geq 1$ GPa display similar spectral evolution, and HMX is observed to decompose from the β-form. Figure 2 shows the spectral evolution of the HMX asymmetric CH_2 stretch under ambient pressure between 178.4 and 186.1 °C. Here the change in peak position and profile between β- and δ-HMX is evident. The peak amplitude for each polymorph is plotted as a function of temperature in Figure 3; it is clear that at ambient pressure (and slow heating rates), β-HMX undergoes complete transformation to δ-HMX prior to decomposition. Experiments conducted at pressures between ambient pressure and 1 GPa show some β-HMX decomposition prior to and during the $\beta \rightarrow \delta$ transformation.

In many of the experiments, product species could be observed. The most frequently observed product peaks appeared at 2225 and 2350 cm^{-1} and are tentatively assigned to N_2O and CO_2. The appearance and relative population of these peaks from one experiment to the next were erratic, partially because of the fact that diamond absorbs close to this region of the spectrum. However, an analysis of the experiments where the products were observed indicates that their formation rates are directly correlated with the decay of the parent HMX peaks. These results indicate that all of the reactions that make up the decomposition of HMX are faster than our instrument response time and that the kinetics of the parent molecule can reasonably represent the global kinetics of the material decomposition.

In all experiments, the peak amplitude for the CH_2 asymmetric stretch was used to monitor the population of HMX as a function of temperature. As a proof of principle, the HMX population was monitored using a variety of peaks in the lower wavenumber region of the spectrum, and the decomposition rate was nearly identical for all peaks. Because of spectral congestion, these lower wavenumber peaks are more difficult to isolate, especially when both β- and δ-HMX are present. Consequently, the asymmetric CH_2 stretch was used to monitor all HMX decompositions reported here. The peak amplitude at each pressure and temperature was normalized to reflect the fraction of reacted HMX for each experiment. Figure 4a shows the fraction reacted as a function of temperature at six different pressures, all at a 0.5 °C/min heating rate; Figure 4b shows the fraction reacted at four different pressures, all at a 0.25 °C/min heating rate. In both parts of Figure 4, it is evident there are two regimes with different trends. At relatively low pressures, that is, between ambient and ca. 1 GPa, raising the pressure lowers the decomposition temperature. At relatively high pressures, that is, $P > 1$ GPa, raising the pressure raises the decomposition temperature.

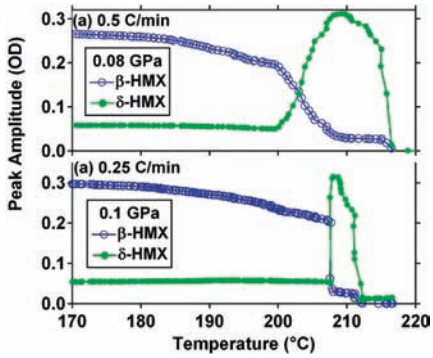

Figure 5. Peak amplitude ($\nu_{as\text{-}CH}$) of β- and δ-HMX at 0.08 and 0.1 GPa. The initial decay of β-HMX (with no corresponding rise of δ-HMX) is attributed to the $\beta \rightarrow$ product reaction. The concomitant decay of β-HMX and rise of δ-HMX corresponds to the $\beta \rightarrow \delta$ transition. The decay of δ-HMX is attributed to the $\delta \rightarrow$ product reaction. The $\beta \rightarrow$ product and $\delta \rightarrow$ product reactions were used to construct the orange curves in Figure 4.

As discussed above, under ambient pressure, HMX decomposes from the δ-polymorph, whereas at elevated pressures (ca. $P > 0.3$ GPa), HMX decomposes from the β-form.[9] In Figure 4a,b, the polymorph of HMX undergoing decomposition is clearly labeled, and most of the curves represent one polymorph of decomposition exclusively. However, at relatively low pressures (i.e., between ambient and 1 GPa), HMX can partially decompose in the β-form (i.e., $\beta \rightarrow$ products reaction) prior to undergoing a polymorph transformation to the δ-form; consequently, it is possible to monitor both β- and δ-HMX decomposition at the same pressure. Figure 5a shows the peak amplitude for both β- and δ-HMX (ca. 3026 and 3057 cm^{-1}, respectively) at 0.08 GPa. In both curves, the β-HMX peak amplitude decreases without any change in the amplitude of the δ-HMX peak; this is indicative of a $\beta \rightarrow$ products reaction (which is a multistep reaction, however, our time resolution does not allow for investigation of any intermediate steps). At 203 °C, the decay of the β-HMX peak accelerates, and there is a concomitant rise in the amplitude of the δ-HMX peak, which is indicative of a $\beta \rightarrow \delta$ polymorph transition. The δ-form lingers briefly and starts to decay, presumably because of the $\delta \rightarrow$ products reaction (which is actually a multistep reaction). The same general trend is observed in Figure 5b at 0.1 GPa, however, the $\beta \rightarrow \delta$ transition occurs at a higher temperature (because of the elevated pressure) and is considerably faster. In contrast, Figure 3 shows the ambient-pressure peak amplitudes for both β and δ-HMX; it is clear that the $\beta \rightarrow \delta$ polymorph transformation occurs prior to any decomposition reactions of β-HMX.

In Figure 4a, the 0.08 GPa curve corresponds to the $\beta \rightarrow$ products and $\delta \rightarrow$ products reactions (i.e., exclusively decomposition and the polymorph transition dynamics are excluded from the figure); the early decomposition is due to β-HMX, and the late decomposition is due to δ-HMX. The 0.1 GPa curve in Figure 4b underwent a similar decomposition pathway; the demarcation between $\beta \rightarrow$ products and $\delta \rightarrow$ products reactions is at the point where the curve steepens (i.e., 0.35 fraction reacted, 209 °C). Figure 4b also shows a curve labeled <1 GPa (purple curve) in which HMX decomposed exclusively in the β-form, and no δ-HMX was ever observed in the experiment. The pressure in this experiment was not well resolved; however, we expect the pressure to be between 0.3 and 1 GPa because of the lack of any δ-HMX peak amplitude and the design of the experiment. Most notable about this curve is its shape: decomposition proceeds at a reasonable rate and then, at 213 °C, suddenly accelerates and is complete in just a few minutes. It is unlikely that the sudden change in decomposition is due to a pressure vent because one would expect a sudden drop in pressure to halt or slow the decomposition rather than accelerate it. In addition, trapped gases were present and observed to form throughout the experiment, and a pressure vent should allow such gases to escape. These curves will be discussed more fully in the discussion section and provide some insight into the role of the polymorph in the decomposition kinetics of HMX.

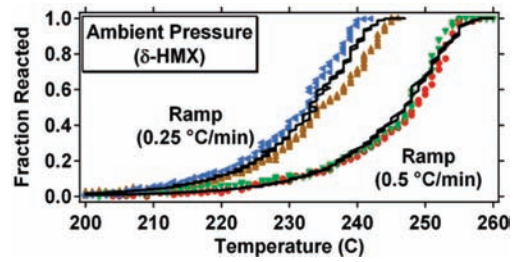

Figure 6. Kinetic model fits (black lines) using the e-PT model to the raw data (colored points) corresponding to ambient pressure, δ-HMX decomposition.

Kinetic Analysis. Arrhenius-based thermal decomposition rates were determined by fitting data from multiple heating rates at the same pressure. A nucleation and growth global kinetic model based on the extended-Prout−Tompkins (e-PT) model[18,19] was chosen. The e-PT model is shown in eq 1

$$dx/dt = (Ae^{-E/RT})(1 - x)^n(1 - q(1 - x))^m \qquad (1)$$

where x is the fraction reacted, E is the activation energy, R is the gas constant, T is temperature, A is the prefactor, and n, m, and q are unitless variables associated with the reaction order, autocatalysis, and nucleation, respectively. The e-PT model is appropriate for modeling the kinetics of autocatalytic decomposition such as that of HMX.[5,20] Piermarini et al. used the Avrami−Erofeev model to determine the kinetics of HMX decomposition in their experiments.[9] Burnham et al. demonstrated that the Avrami−Erofeev and the e-PT models are numerically similar,[21] indicating that the results of our kinetic analysis can be compared with those of Piermarini et al. Our data were fit to the e-PT model using the LLNL program Kinetics05,[22] which numerically integrates the e-PT equation through the exact thermal history.

Because of experimental challenges, reproducing the same pressure to within a few tenths of a gigapascal in a dynamic decomposition experiment for multiple heating rates is extremely difficult; consequently, our study is limited to four key pressure points (ambient pressure, 0.09, 1.1, and 3.6 GPa), which are the average pressures of multiple experiments. In the case of the 0.09 GPa data, there was insufficient data for a kinetic analysis of the β-polymorph, but there was enough data for a kinetic analysis of the δ-polymorph decomposition. Fits to the raw data are shown in Figures 6−9, and the fit parameters are listed in Table 1. The decomposition rate was calculated at 285 °C and compared with the decomposition rate reported by Piermarini et al.[9] at the same temperature. The natural log of the decomposition rates at $T = 285$ °C is plotted as a function of pressure in Figure 10. The decomposition rates at 290 and 300 °C were calculated and are reported in Table S1 of the Supporting Information. These higher temperature rates show a similar overlap with the rates reported by Piermarini et al.[9]

One limitation of the e-PT model is the number of independent variables; one variable could compensate for another in

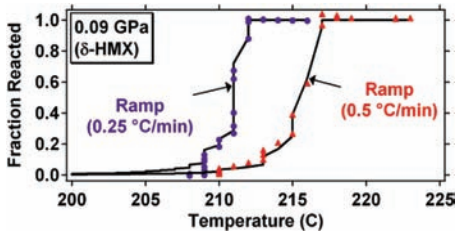

Figure 7. Kinetic e-PT model fits (black lines) to the raw data (colored points) corresponding to 0.09 GPa δ-HMX decomposition. Note that both sets of data originate from experiments where the sample began to decompose in the β-form and underwent a $\beta \rightarrow \delta$ polymorph change and completed decomposition in the δ-form. (Refer to Figure 4.) The data shown here correspond to the fraction of δ-HMX decomposition only and not the total HMX decomposition (i.e., β-HMX decomposition is excluded).

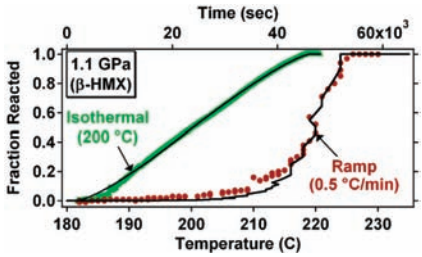

Figure 8. Kinetic e-PT model fits (black lines) to the raw data (colored points) corresponding to 1.1 GPa, β-HMX decomposition.

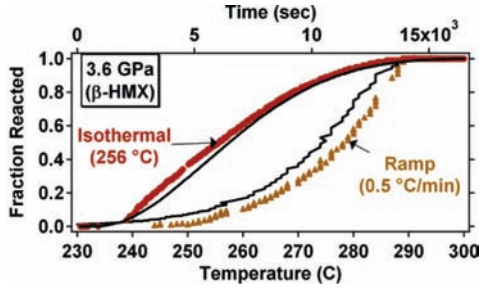

Figure 9. Kinetic e-PT model fits (black lines) to the raw data (colored points) corresponding to 3.55 GPa, β-HMX decomposition.

some cases. As such, we fit the data using fixed values of q and found only marginal differences in the other parameters. We fixed the value of n to 0.5, which is the average value of n in the unrestricted fits, and the value of q to 0.99, which is the best fit value for q in the unrestricted fits, and fit the remaining three parameters (A, E, and m) and found that they were similar to those reported in Table 1. (Refer to Table S2 in the Supporting Information.) The kinetic compensation effect outlined by Brill et al.[5] was tested with our fit parameters by plotting $\ln(A)$ versus E for every fit (i.e., all pressures; fixed and unrestricted fits). In all cases, our e-PT model results match well with literature values compiled by Brill et al.[5] and deviated from Brill's kinetic compensation regression line by only 5−13%. (Refer to Figure 11.) The agreement of our data with the kinetic compensation regression line indicates that the fit parameters and the derived decomposition rates accurately represent the decomposition nature of HMX at the designated pressures.

An analysis of our data was performed using the isoconversional method by Friedman.[23] The isoconversional analysis allows for a calculation of the activation energy (E) and $\ln(Ax^n)$ (A is the Arrhenius prefactor, x is the fraction reacted, n is the reaction order) without assigning a reaction model. The activation energy and $\ln(Ax^n)$ are plotted as a function of fraction reacted at each pressure and are shown in Figures S1 and S2 of the Supporting Information. The average value for E and $\ln(Ax^n)$ at each pressure is reported in Table 2. In general, the average values represent the decomposition parameters accurately; only the 0.09 GPa data show any significant fluctuation. Most importantly, the average activation energy shows the same trend and similar values to those calculated using the e-PT model.

We calculated a fraction-dependent decomposition rate using the isoconversional method by assigning a unimolecular decomposition model (i.e., $n = 1$) and a temperature of 285 °C. The average rates are reported in Table 2, and the fraction/pressure-dependent rates are shown in Figure 12. The advantage of this method is that all of the pressure-dependent data can be compared using a single/identical parameter assumption (i.e., $n = 1$). Both the isoconversional analysis and the e-PT analysis methods produce the same pressure-dependent trend in decomposition rates; however, the actual values are quite different. The $\ln(A)$ versus E pairs from the isoconversional analysis fit well with Brill's kinetic compensation regression line. (Refer to Figure 11.)[5]

Discussion

The main finding of our high-pressure decomposition study is that pressure accelerates HMX decomposition at low-to-moderate pressures (i.e., ambient up to 1 or 2 GPa) and decelerates decomposition at higher pressures (i.e., greater than ca. 2 GPa). The fractional decomposition curves in Figure 4a clearly show that the onset of decomposition shifts as a function of pressure: at 0.08 and 1 GPa, HMX decomposes at temperatures well below the ambient pressure decomposition temperature, and at 2.3 GPa and above, HMX decomposes at temperatures above the ambient pressure decomposition temperature. Two different methods of kinetic analysis of our data indicate that the rate of decomposition accelerates up to 0.09 GPa and decelerates at some pressure >0.09 GPa. (The true inflection point may not be 0.09 GPa, but given our range of data points, 0.09 GPa is a reasonable approximation of the true inflection point.) The comparison of our e-PT decomposition rates with literature values by Burnham et al.[8,24] and Piermarini et al.[9] shows excellent agreement, as shown in Figure 10 and Table 1. Neither Burnham nor Piermarini's study was able to show this inflection in the pressure-dependent decomposition kinetics because the two studies investigated different pressure regimes and employed different methods (DSC vs DAC) and different polymorphs of HMX (δ vs β). However, these studies in combination with our work irrefutably demonstrate this pressure-dependent trend in the decomposition kinetics of HMX and strengthen each study's conclusions.

The change in the global decomposition kinetics, in particular, the pressure-dependent change from acceleratory to deceleratory, is attributed to two different mechanisms driving the decomposition kinetics. It is well established that at ambient pressure, the decomposition of HMX involves heterogeneous, autocatalytic reactions; that is, reactive gases, which are produced through the breakdown of HMX, accelerate the decomposition of the starting material and transient species.[5,20,25] It is also well established that pressure will increase the collision frequency of gaseous species and thus accelerate gas-phase and heterogeneous reactions.[26] We hypothesize that the acceleration in HMX decomposition, up to 0.09 GPa, is due to the enhancement of these heterogeneous and autocatalytic reactions.

The deceleration of HMX decomposition at higher pressures could be attributed to pressure hindering the decomposition initiation step or to pressure changing the mechanism(s) of decomposition. In a study by Naud and Brower,[1] HMX was

TABLE 1: Kinetic Model Fit Parameters for HMX Decomposition at Various Pressures Using the Extended-Prout−Tompkins Global Kinetic Model

pressure (GPa)	k (1/s)[a]	A (1/s)[b]	E (kcal/mol)[b]	m[b]	n[b]	q[b]	exptl method[c]	polymorph of HMX	ref
1.0×10^{-4}	0.008	5.50×10^{10}	32.9	0.25	0.51	0.9999	DSC	δ	[d]
7.0×10^{-3}	0.210	2.83×10^{12}	33.6	1.19	0.77	0.9999	DSC	δ	[e]
1.0×10^{-4}	0.005	7.31×10^{7}	26.1	0.64	0.41	0.99	DAC	δ	this work
0.09	200	9.94×10^{31}	75.9	1.26	0.34	0.99	DAC	δ	this work
1.1	10	1.96×10^{31}	77.3	0.31	0.26	0.99	DAC	β	this work
3.6	0.001	1.61×10^{10}	33.5	0.46	0.64	0.99	DAC	β	this work
3.6	0.0016	NA	NA	NA	NA	NA	DAC	β	[f]
4.6	0.0006	NA	NA	NA	NA	NA	DAC	β	[f]
5.5	0.0003	NA	NA	NA	NA	NA	DAC	β	[f]

[a] Global decomposition rate calculated using the Arrhenius equation at a temperature of 285 °C. Rates calculated in this work are apparent rates and include uncertainty associated with pressure and temperature variability between experiments. [b] Model parameters for the extended-Prout−Tompkins model: $dx/dt = (Ae^{-E/RT})(1 - x)^n(1 - q(1 - x))^m$, where x is the fraction reacted, E is the activation energy, R is the gas constant, T is temperature, A is the prefactor, and n, m, and q are unitless variables associated with the reaction order, autocatalysis, and nucleation, respectively. [c] DSC: differential scanning calorimetry; DAC: diamond anvil cell. [d] Ref 24. [e] Ref 8. [f] Decomposition rate estimated from Figure 8 of ref 9.

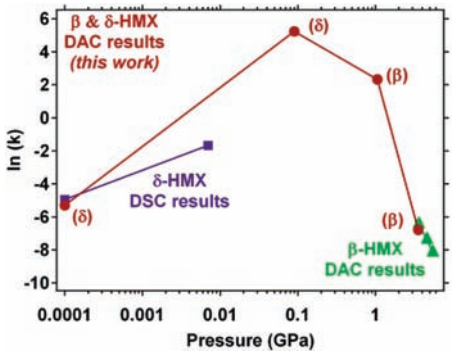

Figure 10. Pressure-dependent reaction rates for HMX decomposition. Red circles correspond to DAC results from this work. Purple squares correspond to DSC results presented by Burnham et al.[8,24] and green triangles correspond to DAC results presented by Piermarini et al.[9] Lines are guides to the eye. All rates correspond to the Arrhenius rate calculated at 285 °C based on the activation energy and Arrhenius prefactor determined from the extended-Prout−Tompkins method. See Table 1 for all extended-Prout−Tompkins values.

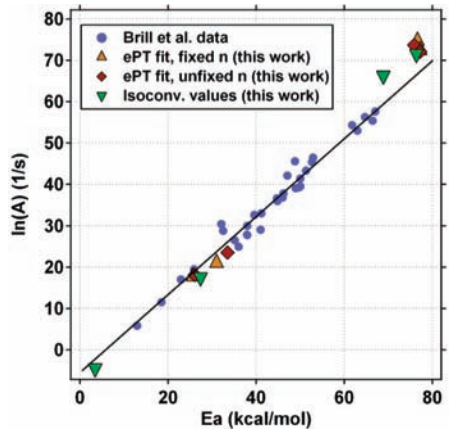

Figure 11. HMX thermal decomposition kinetic compensation plot. Brill et al. data from Table 1 in ref 5.

dissolved in acetone, and the decomposition rate of HMX was monitored at various pressures ranging from ambient to 100 MPa. Dissolving the HMX in acetone inhibited intermolecular reactions and quenched the reactive transient species (e.g., NO_2), and thus Naud and Brower were able to monitor the initiation steps in decomposition without the complications of heterogeneous and autocatalytic reactions. Their study clearly shows that pressure hinders and decelerates decomposition between ambient and 100 MPa. They concluded that the first step in the decomposition of HMX has a positive activation volume, and they hypothesized that the reaction begins with HONO elimination, N−NO_2 bond homolysis, or both. Taking into consideration the results of Naud and Brower's work, it is possible that the deceleration in HMX decomposition that we observe in our solid-state study is also due to pressure hindering the initiation step(s). It is also possible that pressure hinders HMX decomposition by hindering the creation of one or more of the transient species in the reaction. The phase (i.e., liquid vs gas) of the transient species and initial decomposition products at different pressures may change the decomposition mechanism(s).

We hypothesize that the competing effects of pressure on the decomposition of HMX are occurring over the full range of pressures in our study; however, one mechanism dominates over the other at different pressure regimes. As one raises the pressure, the initial decomposition of HMX is hindered, however, a sufficient population decomposes resulting in reactive gases which accelerate the decomposition, and the rate is determined by the degree of autocatalysis. At the true inflection point pressure hinders the initiation step so much that the rate is determined by the rate of HONO and/or N-NO_2 bond homolysis.

The role and influence of the HMX polymorph in the decomposition kinetics of HMX is a more difficult topic of study because the decomposition is complex, and decomposing β- and δ-HMX under similar conditions is difficult. Figure 4a,b shows β- and δ-decomposition of HMX at low pressures (i.e., < 1 GPa). In the experiments at ca. 0.08 and 0.1 GPa, the sample begins to decompose in the β-form, then undergoes a rapid and complete polymorph transformation to the δ-form, and completes decomposition from the δ-polymorph. There was insufficient data for a kinetic analysis of the β-polymorph, but there was enough data for a kinetic analysis of the δ-decomposition. Kinetic analysis using the extended-Prout−Tompkins method clearly indicates that the δ-polymorph decomposition at 0.09 GPa is faster than the β-decomposition at 1.1 GPa, yet relative to the decomposition at ambient pressure or 3.6 GPa, both are quite fast. One should take care, however, in relying too heavily on this quantitative data from the 0.09 GPa δ-decomposition because the reaction was quite fast and only about 15 data points/curve were used to analyze the kinetics. Kinetic analysis using the isoconversional analysis indicates that all of the decomposition parameters (i.e., activation energy, $\ln(Ax^n)$, and rate) of δ-HMX at 0.09 GPa are similar to, but considerably more variable, than those of β-HMX at 1.1 GPa. More work is

TABLE 2: Average Kinetic Parameters for HMX Decomposition at Various Pressures Using the Friedman Isoconversional Analysis[a]

pressure (GPa)	E (kcal/mol)[b]	$\ln(Ax^n)$[b]	k (1/s)[c]	A (1/s)[d]	exptl method[e]	polymorph of HMX
1.0×10^{-4}	3.4	−4.8	2.26×10^{-3}	9.98×10^{16}	DAC	δ
0.09	68.9	65.3	3.16×10^{6}	1.38×10^{75}	DAC	δ
1.1	76.4	70.7	5.70×10^{4}	6.07×10^{79}	DAC	β
3.6	27.4	16.8	8.87×10^{-4}	3.00×10^{14}	DAC	β

[a] All values are averaged between the fraction reacted range of 0.2 and 0.8. [b] Parameters for Friedman isoconversional analysis; E is the activation energy, A is the Arrhenius prefactor, x is the fraction reacted, and n is the reaction order. Refer to Figures S1 and S2 of the Supporting Information for complete data sets. [c] Decomposition rate calculated using the Arrhenius equation at a temperature of 285 °C and assigning a reaction order of $n = 1$. [d] Arrhenius prefactor calculated with a reaction order of $n = 1$. [e] DAC: diamond anvil cell.

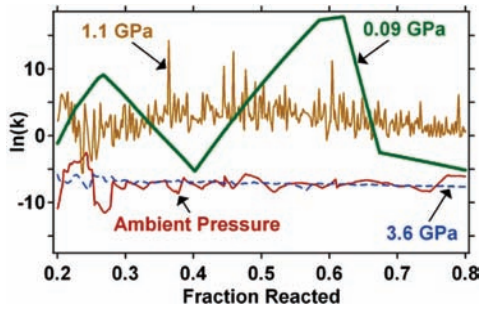

Figure 12. Pressure-dependent reaction rates for HMX decomposition at $T = 285$ °C based on the isoconversional analysis assuming unimolecular decomposition. See Table 2 for the complete isoconversional analysis results.

necessary to draw any firm and quantitative conclusions about the kinetics of β- versus δ-HMX.

In addition to a quantitative comparison, a qualitative analysis provides some insight into the relative decomposition rates of β- versus δ-polymorphs. Comparison of the shape of the β- and δ-polymorph decomposition curves at 0.08 and 0.1 GPa is interesting. (See Figure 4.) In both experiments, the β-HMX curve has a gentle slope, and the δ-HMX curve has a very steep slope. This may indicate that in these two experiments, δ-HMX decomposes faster than β-HMX, yet the <1 GPa curve in Figure 4b shows a similar change in slope when the sample decomposed exclusively in the β-polymorph. It is possible that the sudden change in slope in the <1 GPa curve results from a rapid and sequential $\beta \rightarrow \delta \rightarrow$ product decomposition mechanism, where the δ-polymorph may be unobservable because of our ca. 1 min time resolution and instrument sensitivity. It is also possible that the acceleration is due to enhanced autocatalysis and not a change in mechanism or an inherent change in the chemical kinetics of one polymorph versus the other. The data presented here are insufficient to make a definitive statement about whether β- or δ-HMX decomposes more rapidly under identical conditions; however, the results clearly indicate that both polymorphs are sensitive to pressure during thermal decomposition.

Summary

The results of this study further elucidate the pressure-dependent thermal decomposition process starting from β- or δ-HMX. A global decomposition rate inflection point was found in the 100 MPa regime. The decomposition rate dependence on pressure is attributed, although not limited, to the competing effects of autocatalysis, which is enhanced with pressure, and reaction initiation, which is hindered by pressure. These results allow for a more confident assessment of the thermal safety of HMX-based materials and will guide in the interpretation of multivariable cook-off experiments. Further work is underway to investigate some of the remaining questions concerning the pressure-dependent decomposition kinetics of HMX.

Acknowledgment. We thank J. L. Maienschein for helpful discussion and Sabrina DePiero for supplying the samples. This work performed under the auspices of the U.S. Department of Energy by Lawrence Livermore National Laboratory under contract DE-AC52-07NA27344.

Supporting Information Available: Extended-Prout−Tompkins-based reaction rates at different temperatures and model fit parameters with fixed values for n and q and isoconversional analysis results (E and $\ln(Ax^n)$) of HMX decomposition. This material is available free of charge via the Internet at http://pubs.acs.org.

References and Notes

(1) Naud, D. L.; Brower, K. R. *J. Org. Chem.* **1992**, *57*, 3303.
(2) Chakraborty, D.; Muller, R. P.; Dasgupta, S.; Goddard, W. A., III. *J. Phys. Chem. A* **2001**, *105*, 1302.
(3) Behrens, R., Jr. Thermal Decomposition Processes of Energetic Materials in the Condensed Phase at Low and Moderate Temperatures. In *Overviews of Recent Research on Energetic Materials*; Shaw, R. W., Brill, T. B., Thompson, D. L., Eds.; World Scientific Publishing: Hackensack, NJ, 2005.
(4) Oyumi, Y.; Brill, T. B. *Combust. Flame* **1985**, *62*, 213.
(5) Brill, T. B.; Gongwer, P. E.; Williams, G. K. *J. Phys. Chem.* **1994**, *98*, 12242.
(6) Tarver, C. M.; Tran, T. D. *Combust. Flame* **2004**, *137*, 50.
(7) Wemhoff, A. P.; Howard, M. H.; Burnham, A. K.; Nichols, A. L., III *J. Phys. Chem. A* **2008**, *112*, 9005.
(8) Burnham, A. K.; Weese, R. K.; Wardell, J. F.; Tran, T. D.; Wemhoff, A. P.; Koerner, J. G.; Maienschein, J. L. *Proceedings of the 13th International Detonation Symposium*, Norfolk, VA, Office of Naval Research, 2006; p 573.
(9) Piermarini, G. J.; Block, S.; Miller, P. J. *J. Phys. Chem.* **1987**, *91*, 3872.
(10) Henson, B. F.; Smilowitz, L.; Asay, B. W.; Sandstrom, M. M.; Romero, J. J. *Proceedings of the 13th International Detonation Symposium*, Norfolk, VA, Office of Naval Research, 2006; p 778.
(11) Lee, E. R.; Sandborn, R. H.; Stromberg, H. D. *Proceedings of the 5th International Detonation Symposium*, Pasadena, CA, Office of Naval Research, 1970; p 331.
(12) Maienschein, J. L.; Wardell, J. F.; DeHaven, M. R.; Black, C. K. *Propellants, Explos., Pyrotech.* **2004**, *29*, 287.
(13) Wardell, J. F.; Maienschein, J. L. *Proceedings of the 12th International Detonation Symposium*, San Diego, CA, Office of Naval Research, 2002; p 384.
(14) Datchi, F.; LeToullec, R.; Loubeyre, P. *J. Appl. Phys.* **1997**, *81*, 3333.
(15) Montgomery, W.; Zaug, J. M.; Howard, M. H.; Goncharov, A. F.; Crowhurst, J. C.; Jeanloz, R. *J. Phys. Chem. B* **2005**, *109*, 19443.
(16) Landers, A. G.; Brill, T. B. *J. Phys. Chem.* **1980**, *84*, 3573.
(17) Brand, H. V.; Rabie, R. L.; Funk, D. J.; Diaz-Acosta, I.; Pulay, P.; Lippert, T. K. *J. Phys. Chem. B* **2002**, *106*, 10594.
(18) Burnham, A. K.; Braun, R. L. *Energy Fuels* **1999**, *13*, 1.
(19) Burnham, A. K.; Weese, R. K.; Wemhoff, A. P.; Maienschein, J. L. *J. Therm. Anal.* **2007**, *89*, 407.
(20) Behrens Jr., R.; Margolis, S. B.; Hobbs, M. L. *Proceedings of the 11th International Detonation Symposium*, Snowmass, CO, Office of Naval Research, 1998; p 533.
(21) Burnham, A. K.; Braun, R. L.; Coburn, T. T.; Sandvik, E. I.; Curry, D. J.; Schmidt, B. J.; Nobel, R. A. *Energy Fuels* **1996**, *10*, 49.

(22) Braun, R. L.; Burnham, A. K. *Kinetics05*; The Regents of the University of California: Livermore, CA, 2006.
(23) Friedman, H. L. J. *Polym. Sci. Part C* **1964**, *6*, 183.
(24) Burnham, A. K.; Weese, R. K. *Proceedings of the 36th International ICT Conference and 32nd International Pyrotechnics Seminar*, Karlsruhe, Germany, 2005; p 1.
(25) Behrens, R., Jr.; Bulusu, S. *Proceedings of the Fourth International Symposium on Special Topics in Propulsion*, 1996; p 278.
(26) McQuarrie, D. A.; Simon, J. D. *Physical Chemistry: A Molecular Approach*; University Science Books: Sausalito, CA, 1997.

JP905276K